ELSEVIER

Journal of Alloys and Compounds 323–324 (2001) 494–497

Journal of ALLOYS AND COMPOUNDS

www.elsevier.com/locate/jallcom

Raman phonons and light scattering in $RMnO_3$ (R=La, Pr, Nd, Ho, Er Tb and Y) orthorhombic and hexagonal manganites

L. Martín-Carrón*, A. de Andrés, M.J. Martínez-Lope, M.T. Casais, J.A. Alonso

Instituto de Ciencia de Materiales de Madrid, C.S.I.C., Cantoblanco, E-28049 Madrid, Spain

Abstract

$RMnO_3$ compounds present the *Pbnm* orthorhombic structure for R=La, Pr, Nd while compounds with smaller ionic radii (R=Ho, Er Tb and Y) can be obtained either in the *Pbnm* or the $P6_3cm$ hexagonal structure. Their magnetic and transport properties are strongly dependent on the rare earth and, therefore, on their detailed structure. We have studied these compounds through the Raman phonons of both structures as a function of the rare earth ion and temperature. The phonon frequencies of the main peaks of *Pbnm* structure have been correlated to structural characteristics, such as bond-lengths or bond angles, obtained from the analysis of neutron diffraction data. According to the structural and Raman behavior, these compounds can be classified into two groups: one includes La, Pr, and Nd, and the other includes the rest. This classification also correlates to the different behavior of their magneto transport properties when doped. A structural transition to a cubic or quasi-cubic perovskite, above 800 K, can be deduced from the phonon spectra for $YMnO_3$ orthorhombic compound.

Keywords: Magnetically ordered materials; Electron–phonon interactions; Phase transitions; Phonons; Inelastic light scattering

Introduction

Recently $R_{1-x}A_xMnO_3$ (R=rare earth trivalent ion and A=alkaline-earth divalent ion) have attracted much attention due to the colossal magnetoresistance that many of them present [1]. The subtle equilibrium between the different interactions present in the samples determines if they are metallic or insulators, ferro or antiferromagnetically ordered, charge ordered or present phase segregation [2]. The substitution of the rare earth for a divalent cation A gives rise to the appearance of Mn^{4+} ions, introducing holes in the e_g band leading, in some cases, to the metallic and/or ferromagnetic behavior; but even in the absence of doping there can be a certain amount of Mn^{4+} ions due to the so called oxidative non-stoichiometry [3,4]. In these 'non-doped' materials the presence of mixed valences gives rise to the same double exchange mechanism as in doped ones. All these properties are strongly dependent on their detailed structure and, therefore, on the rare earth ion.

$RMnO_3$ compounds crystallize in orthorhombic structure [space group *Pbnm* (D_{2h}^{16}) and $Z=4$] [5,6] for R with larger ionic radius (R=La to Dy), whereas the compounds with R of smaller ionic radius (R=Ho, Er and Y) can be obtained either in the orthorhombic or the hexagonal structure [space group $P6_3cm$ (C_{6v}^3) and $Z=6$] [7]. For the orthorhombic structure the manganese ions are at octahedral sites (MnO_6) while for the hexagonal structures they are in bipyramids (MnO_5).

Stoichiometric $RMnO_{3.00}$ compounds are interesting as they present a static Jahn–Teller distortion, with orbital ordering. The absence of Mn mixed valence determines the insulating character of these samples. J.A. Alonso et al. have studied the dependence of this MnO_6 Jahn–Teller distortion, at room temperature, with the size of the R^{3+} ions [6]. Although there are some articles related to Raman studies in manganites, none of them study the dependence of the Raman spectra with the rare earth and the evolution of the Jahn–Teller distortion. Illiev et al. have observed the Raman active phonons of orthorhombic $LaMnO_3$ and $YMnO_3$ [8], and hexagonal $YMnO_3$ [7], and estimated their frequencies from lattice dynamical calculations. Other authors [9–12] have reported Raman studies on different doped manganites (or undoped $LaMnO_3$), usually with orthorhombic structure, and Abrashev et al. have compared the optical phonons of rhombohedral perovskites $LaMnO_3$ and $LaAlO_3$ [13].

We have studied the Raman phonons of stoichiometric $RMnO_3$, with orthorhombic *Pbnm* structure, as a function

*Corresponding author.

0925-8388/01/$ – see front matter
PII: S0925-8388(01)01047-7

of the rare earth ion and temperature, as well as the Raman phonons of hexagonal $YMnO_3$.

Experimental details

$RMnO_3$ samples with (R=Pr, Nd, Tb, Ho, Er and Y) were all obtained by citrate techniques [6]. For R=Pr and Nd, the precursors were treated at 1100°C in a N_2 flow for 12 h; annealing treatments in an inert atmosphere were necessary to avoid the formation of non-stoichiometric $Pr(Nd)MnO_3$ phases, containing a significant amount of Mn^{4+}. For R=Tb, the precursor powders were heated at 1000°C in air for 12 h. Finally, low temperature treatments were necessary for the samples with R=Ho, Y and Er, to increase the yield of the orthorhombic phases, preventing or minimizing the stabilization of competitive hexagonal $RMnO_3$ phases.

Raman spectra were obtained with a Renishaw Ramanscope 2000 and exciting the samples with the 514.5 and 633 nm lines of Ar and He–Ne lasers. The spectra were recorded in the backscattering geometry. The samples were locally heated at the laser spot depending on the laser power. The local temperature of these samples was estimated taking into account the relative Stokes to anti-Stokes Raman intensities.

Results and discussion

As said before, there are two possible structures depending on the rare earth ionic radius at room temperature (RT), orthorhombic *Pbnm* for larger ionic radius, or hexagonal $P6_3cm$ for smaller ionic radius. The Raman active modes of the *Pbnm* structure (long axis: *c*) are [8]: $7A_g+7B_{1g}+5B_{2g}+5B_{3g}$, while those for the hexagonal $P6_3cm$ structure are: $9A_1+14E_1+15E_2$ [7].

All the samples studied here have the orthorhombic *Pbnm* structure except for the $YMnO_3$ sample labeled H that had the hexagonal $P6_3cm$ structure. In Fig. 1 we show the variation of the unit cell parameters and cell volume with the ionic radius of the rare earth. For the small ionic radii, the variation of the *b* parameter is very small compared to that of *a* and *c*; this is due to the tilting scheme of the MnO_6 octahedra in *Pbnm* perovskites where the distortion, driven by a reduction of the rare earth size, leaves the parameter *b* almost unchanged. For large ionic radii we can observe a change in this cell parameter behavior (Fig. 1). The observed decrease in the unit cell volume scales with the R^{3+} size.

We have compared the Raman spectra at room temperature, for different rare earth parent compounds. The Raman spectra of the orthorhombic compounds are similar but they can be grouped into two kinds of spectra: La, Pr and Nd on one hand, and the rest on the other (Fig. 2); the same classification as the previous one related to *b*-parameter behavior. The modes corresponding to the orthorhombic structure are: A_g+B_{1g} symmetric and $2B_{2g}+2B_{3g}$ antisymmetric stretching modes; $A_g+2B_{1g}+B_{3g}$ bending modes and $2A_g+2B_{2g}+B_{1g}+B_{3g}$ rotation and tilt modes of the octahedra; and $3A_g+B_{2g}+3B_{1g}+B_{3g}$ modes related to the rare earth movements [8]. Among these, the three main peaks correspond to the following modes and symmetries: the symmetric stretching of the basal oxygens

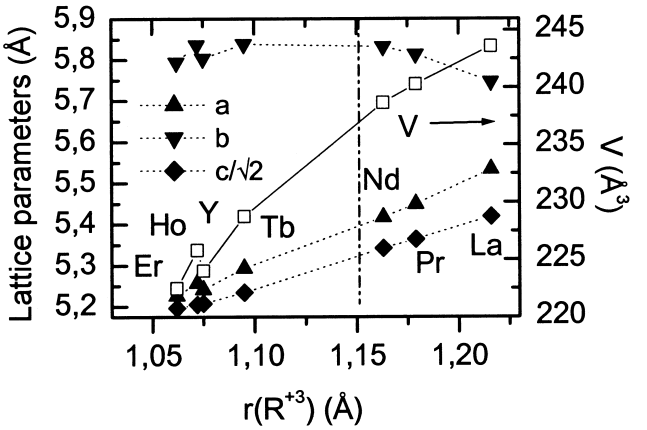

Fig. 1. Variation of the unit cell parameters (left) and volume (right) with the ionic radius of R^{3+}.

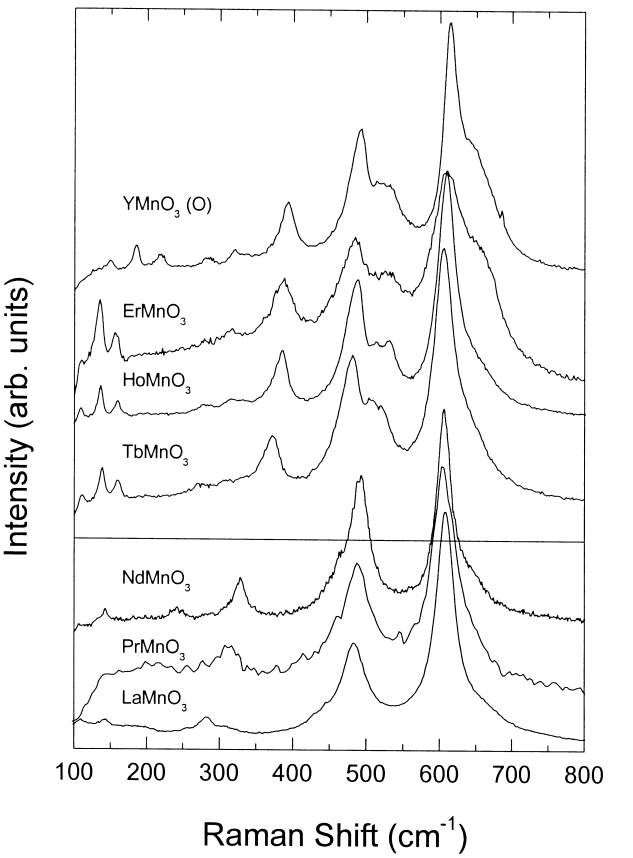

Fig. 2. Raman spectra as a function of the rare earth at RT, for ortho-manganites.

of the octahedra (Fig. 3c), around 610 cm^{-1} (B_{1g} symmetry); the asymmetric stretching at 480 cm^{-1} (A_g symmetry) associated with the Jahn–Teller distortion (Fig. 3b); and the tilt of the octahedra at 280 cm^{-1} (A_g symmetry) Fig. 3a). The modes at lowest energies are those related to the rare earth movements.

The higher frequency mode varies only slightly with the ionic radius (about 10 cm^{-1}) and, as it involves nearly pure Mn–O bond stretchings, a $r^{-1.5}$ dependence of this phonon frequency is expected. This behavior is clearly seen in Fig. 4a, b. In contrast, the peak at about 300 cm^{-1} changes enormously with the rare earth (280 cm^{-1} for La up to 400 cm^{-1} for the smallest radius), and has a proportional variation with the tilt of the octahedra (Fig. 4e), and inverse variation with the cell volume (Fig. 1); that means that this mode is well associated with the hydrostatic pressure of the lattice.

The modes in the 450–550 cm^{-1} region behave in a different way, depending on the size of the rare earth; again, two different groups can be clearly differentiated. For large ionic radii compounds (group of La, Nd and Pr), the frequency of this mode follows the Jahn–Teller distortion (Fig. 4c, d), softening as the distortion decreases; however, for the small ionic radii compounds (group of Y, Er, Ho and Tb) the frequency behavior fits with the Mn–O_2 bond distances. If we now look at the $RMnO_3$ spectra again, we can see that these two different groups of rare earth compounds correspond with the rare

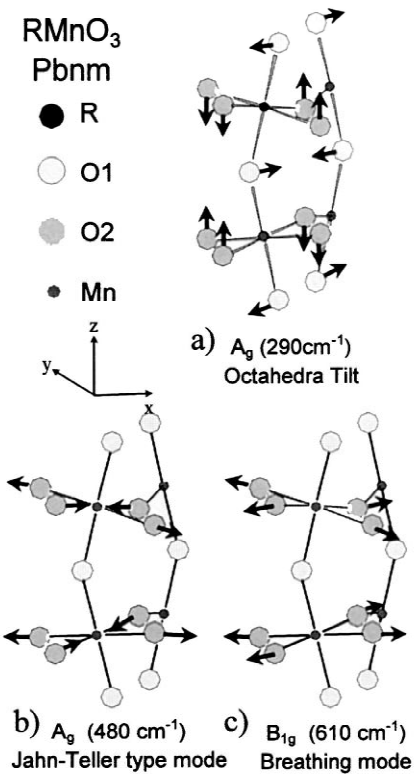

Fig. 3. (a) Octahedra tilt (A_g symmetry); (b) Asymmetric stretching (A_g symmetry); (c) Symmetric stretching (B_{1g} symmetry).

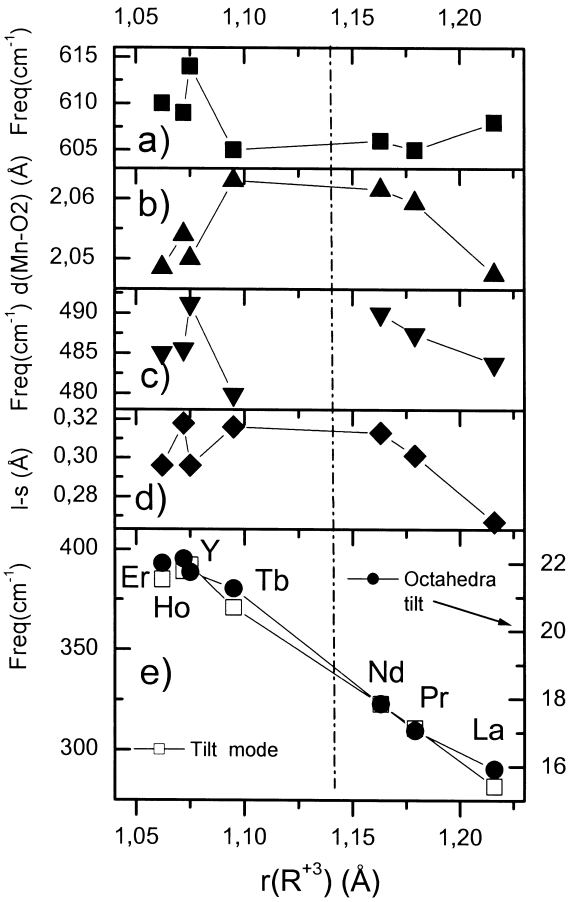

Fig. 4. (a) Dependence of the stretching mode frequency with the ionic radius of $RMnO_3$ at RT. (b) Mean value of the Mn–O_2 distances of the octahedra. (c) Frequency of the Jahn–Teller mode. (d) Jahn–Teller distortion. (e) Frequency of the tilt mode (left) compared with the tilting of the octahedra (right).

earth at which more peaks appear (as expected from factor group analysis) at these frequencies.

In Fig. 5 we present the Raman spectra of a $YMnO_3$ sample that is mostly orthorhombic (with about 12% content of hexagonal phase). In the room temperature Raman spectrum, we observe some peaks that can be assigned to the hexagonal structure. The intensity ratio between the peaks corresponding to both phases is not constant through the sample, so the sample is not homogeneous at a ~2-μm scale (laser spot diameter). As temperature increases, the intensity of the modes associated with the orthorhombic structure decreases and disappears above 800 K while the hexagonal features remain. The inset shows the linear dependence of temperature with laser power, just to check that our method of estimation for the local temperature of the sample is correct. Orthorhombic $LaMnO_3$ [14] presents a phase transition to a pseudocubic structure at high temperature, around 750 K. The explanation for the disappearance of the orthorhombic peaks is that a similar structural transition is happening in the orthorhombic part of the $YMnO_3$ sample, where the Jahn–

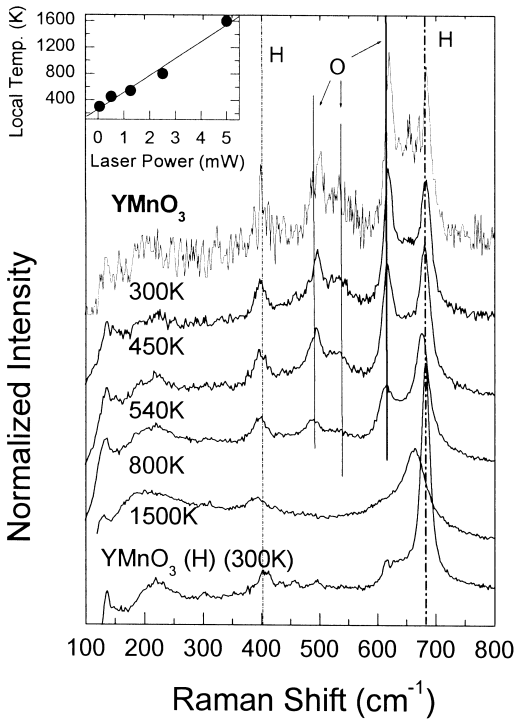

Fig. 5. Raman spectra of a $YMnO_3$ sample with orthorhombic structure as a function of temperature. The Raman spectra of a hexagonal $YMnO_3$ sample are also shown. Inset: linear dependence of the local temperature with laser power.

Teller distortion of the octahedra disappears leading to a nearly cubic perovskite structure. For this structure no Raman peaks are active. The observation of the hexagonal spectrum and the reversibility of the spectra by decreasing the laser power ensures that the sample is not burnt or changed by the laser beam.

Conclusions

In summary, we have studied the Raman active phonons of stoichiometric $RMnO_3$ compounds with orthorhombic structure and compared them to the Raman spectra of a hexagonal $YMnO_3$ sample. We have correlated the frequencies of the three most intense modes of the orthorhombic samples, with some structural parameters such as Mn–O bond distances, octahedra tilt angle and Jahn–Teller distortion.

We have seen that, as the ionic radius of the rare earth decreases, with a consequent reduction of the unit-cell volume and an increase in the tilt angle, the frequency of the mode at 280 cm^{-1} increases dramatically, following a linear dependence with the tilt angle. The stretching mode at 610 cm^{-1} behaves inversely with the mean distances of Mn–O bonds in the basal plane. We correlated the 480 cm^{-1} peak with the Jahn–Teller distortion for compounds with large ionic radii, while it was correlated with the change in the $Mn–O_2$ bond distances for small radii. We also showed how the same classification for rare earth compounds can be made considering structural parameters, such as the cell parameter *b*. This behavior can be noted in the Raman spectra where different number of peaks can be seen, in the frequency range between 480 and 550 cm^{-1}, for small/large R ionic radii.

Finally, we observed that, as temperature increases, the Raman peaks corresponding to the orthorhombic phase of an $YMnO_3$ sample disappear above 800 K, while those corresponding to the hexagonal phase remain. We associate these changes in the spectra to a structural transition of the orthorhombic phase to a cubic or quasi-cubic structure above 800 K.

Acknowledgements

We would like to acknowledge the financial support from CAM07N/0027/1999 and MAT99/1045.

References

[1] S. Jin, T.H. Tiefel, M. McCormack, R.A. Fastnocht, R. Ramesh, L.H. Chen, Science 264 (1994) 413.
[2] Y. Tomika, A. Asamitsu, Y. Morimoto, H. Kuwahara, Y. Tokura, Phys. Rev. Lett. 74 (1995) 5108.
[3] B.C. Hauback, H. Fjelluag, N. Sakai, J. Solid State Chem. 124 (1996) 43.
[4] C.N. Rao, A.K. Cheetham, Science 272 (1996) 369.
[5] H.L. Yakel, W.C. Koehler, E.F. Bertaut, E.F. Forrat, Acta Crystallogr. 16 (1963) 957.
[6] J.A. Alonso, M.J. Martínez-Lope, M.T. Casais, M.T. Fernández-Díaz, Inorg. Chem. 39 (2000) 917.
[7] M.N. Iliev, H.G. Lee, V.N. Popov, M.N. Abrashev, A. Hamed, R. Lmeng, C.W. Chu, Phys. Rev. B 56 (1997) 2488.
[8] M.N. Iliev, M.V. Abrashev, H.G. Lee, V.N. Popov, Y.Y. Sun, C. Thomsen, R.L. Meng, C.W. Chu, Phys. Rev. B 57 (1998) 2872.
[9] V.B. Podobedov, A. Weber, D.B. Romero, J.P. Rice, H.D. Drew, Phys. Rev. B 58 (1998) 43.
[10] E. Granado, N.O. Moreno, A. García, J.A. Sanjurjo, C. Retori, I. Torriani, S.B. Oseroff, J.J. Neumeier, K.J. McClellan, S.W. Cheong, Y. Tokura, Phys. Rev. B 58 (1998) 11435.
[11] E. Liarokapis, T. Leventouri, D. Lampakis, D. Palles, J.J. Neumeier, D.H. Goodwin, Phys. Rev. B 60 (1999) 12758.
[12] V. Dediu, C. Ferdeghini, F.C. Matacotta, P. Nozar, G. Ruani, Phys. Rev. Lett. 84 (2000) 4489.
[13] M.V. Abrashev, A.P. Litvinchuk, M.N. Iliev, R.L. Meng, V.N. Popov, V.G. Ivanov, R.A. Chakalov, C. Thomsen, Phys. Rev. B 59 (1999) 4146.
[14] J. Rodríguez-Carvajal, M. Hennion, F. Moussa, A.H. Moudden, L. Pinsard, A. Revcolevschi, Phys. Rev. B 57 (1998) R3189.